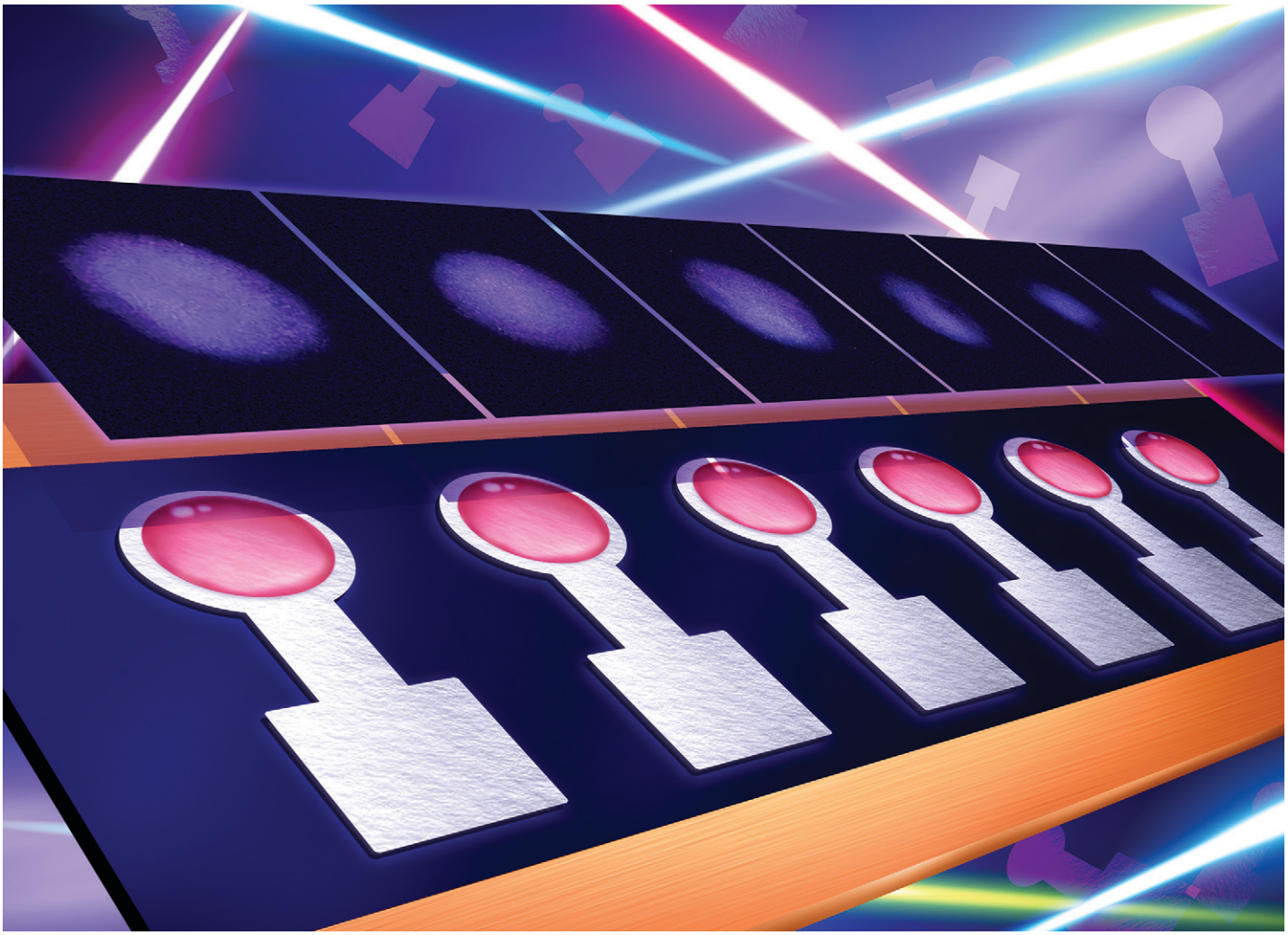

Showcasing research from Professor Garcia's laboratory, Department of Chemistry, Clemson University, Clemson, USA.

From glow-sticks to sensors: single-electrode electrochemical detection for paper-based devices

A novel, portable, and inexpensive sensor for multiplex determinations was developed using a single-electrode electrochemical system, electrochemiluminescence, and paper-based devices. The detection electrode was fabricated using carbon paint and the dye contained in commercial glow sticks was used as the optical reporter. Besides the electrode material, the system was characterized considering the potential applied, the dimensions of the paper device, and the detection step. The system was applied towards the detection of peroxide, including those generated during the oxidation of lipids and those produced by the enzymatic transformation of glucose.

As featured in:

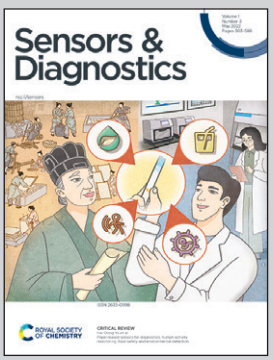

See Carlos D. Garcia *et al.*, *Sens. Diagn.*, 2022, **1**, 496.

ROYAL SOCIETY OF CHEMISTRY

rsc.li/sensors

Registered charity number: 207890

Sensors & Diagnostics

PAPER

View Article Online
View Journal | View Issue

Cite this: *Sens. Diagn.*, 2022, **1**, 496

From glow-sticks to sensors: single-electrode electrochemical detection for paper-based devices†

Ezequiel Vidal, [ab] Claudia E. Domini,[b] Daniel C. Whitehead [a] and Carlos D. Garcia *[a]

With the goal of creating a multipurpose platform for electrogenerated luminescence, a single electrode electrochemical system was designed, developed, and validated. Glow sticks were used as the source of the luminophore, which was used as the optical reporter for the biosensor. A smartphone was used as the detector to quantify the electrochemiluminescence emissions. A disposable paper-based device was designed and used as a two-compartment electrochemical reaction cell, affording the possibility to individually optimize the sensing and detection reactions. This sensor assembly was tested under different conditions, showing acceptable performance both in the determination of hydrogen peroxide concentrations, to evaluate rancidity markers in edible oil samples, and to quantify the glucose concentration in soft drinks. The analytical performance of the single electrode, electrochemiluminescent device showed a limit of detection for hydrogen peroxide of 1.02 μM, with a working range between 0.4 μM and 150 mM. The proposed approach represents the first example of a system that combines paper-based devices, single electrode electrochemistry, electrochemiluminescence, and smartphone image sensing. As such, it not only provides a convenient platform for the development of a variety of analytical applications but also broaden the versatility of ePADs.

Received 14th March 2022,
Accepted 7th April 2022

DOI: 10.1039/d2sd00041e

rsc.li/sensors

1. Introduction

A survey of the recent literature shows that while the versatility of biosensors continues to increase,[1–3] most of them only allow the determination of a single analyte[4–6] often requiring the inclusion of additional technologies to obtain a comprehensive metabolite coverage.[7–9] On the other hand, the development of multiplex assays (*i.e.* those that allow simultaneous analysis in a single run[10,11]) presents a new set of analytical opportunities and can not only provide a more complete description of the sample but also minimize analysis time and cost.[12,13] Towards these goals, a wide variety of detection methodologies have been implemented in multiplex systems, including colorimetry, fluorescence,[14,15] surface plasmon resonance,[16,17] electrochemistry,[17,18] and chemiluminescence.[19,20] Although each of these strategies offer specific advantages, these detection systems often require specific instrumentation and operating parameters, which limit their application. Alternatively, electrochemiluminescence (ECL, also known as electrogenerated chemiluminescence) has emerged as one of the simplest, most sensitive, and versatile detection platforms that has been applied for a wide range of analytes.[21–24] ECL refers to the electrochemical generation of species (*i.e.* a luminophore and co-reactant) that then react to form secondary species in excited states which finally decay and emit light.[25] While the most used luminophores are based on the use of luminol[26] or $Ru(bpy)_3^{2+}$,[27] a variety of metallic complexes and polyaromatic hydrocarbons have also been reported.[25,28] It is also important to consider that ECL has been coupled with traditional electrochemical approaches such as amperometry[29–31] as well as bipolar systems.[6,21,26,32–34] While not strictly considered a bipolar system, ECL can also be integrated with much simpler electrochemical systems that use a single, resistive electrode[33] to drive a potential drop across the detection cell.[35–37] This approach, often referred to as single electrode electrochemical systems (SEES),[21,33,38,39] can be implemented using a variety of substrates including ITO[38] or carbon-based systems,[21,40] and hold great promise for bioanalytical applications.[21,33,38,39]

Considering the recent expansion of low-cost analytical platforms, this paper describes the possibility to couple SEES and ECL with paper-based analytical devices (PADs). Unlike

[a] *Department of Chemistry, Clemson University, 211 S. Palmetto Blvd., Clemson, SC, 29634, USA. E-mail: cdgarci@clemson.edu; Tel: +(864) 656 1356*
[b] *INQUISUR, Departamento de Química, Universidad Nacional del Sur (UNS)-CONICET, Av. Alem 1253, 8000, Bahía Blanca, Argentina*

† Electronic supplementary information (ESI) available. See DOI: https://doi.org/10.1039/d2sd00041e

ePADs (mostly based on amperometry) or traditional SEES (where the redox species are mixed and in direct contact with the electrode), this paper describes the possibility to use a dumbbell-shaped paper device that allows separating the anodic and cathodic reactions, using individually-optimized reaction conditions. To maximize access to the platform, carbon paint was used as the electrode material and the dye contained in commercial glow sticks was used as the optical reporter. The operation and performance of the proposed system was investigated using standard solutions of hydrogen peroxide and the applicability of the approach was demonstrated by measuring lipid peroxides in edible oils and glucose (*via* glucose oxidase) in soft drinks and fruits. To the best of our knowledge, this study represents the first demonstration of the use of paper-based devices coupled with a single-electrode electrochemical system. This combination along with detection using a smartphone provides a convenient platform for the expansion of detection schemes applied to μPADs.

2. Experimental section

Materials and methods

Aqueous solutions were prepared in deionized water (MilliQ, Millipore water systems; Billerica, MA, USA). Citrate buffer (0.1 M; pH = 6.0) was prepared using sodium citrate dihydrate (Sigma-Aldrich, St. Louis, MO) and citric acid (Aldrich Chemical Co. LLC, Milwaukee, WI), adjusting the pH with 0.1 M HCl and measuring the pH with a glass electrode and a digital pH meter (Orion 420A+, Thermo; Waltham, MA). A 30% aqueous solution of hydrogen peroxide was purchased from Fisher BioReagents (Merelbeke, Belgium), and α-D-glucose was obtained from Aldrich Chemical Co. LLC (Milwaukee, WI). Glucose oxidase from *Aspergillus niger* (≥15 000 units per g, 160 kDa, isoelectric point 4.2) was purchased from Sigma-Aldrich. In all cases, the electrolyte solution was prepared to contain 0.2 M NaOH (Acros Organics, Geel, Belgium), 1 M KCl (EM Science, Gibbstown, NJ), and 0.2 M Triton-X (Aldrich Chemical Co. LLC, Milwaukee, WI). The surfactant was added to the electrolyte to facilitate the contact between the aqueous solution and the carbon electrode as well as to enhance the ECL.[41]

Glow sticks (Glow; Irving, TX, USA) were purchased at a local store and were carefully disassembled to extract the dye, contained in the inner glass ampule.[42,43] In order to rationally approach the utilization of the glow sticks, the chemical composition and optical properties of the dye contained within were investigated by a combination of thin-layer chromatography, HPLC-MS (Agilent 6545 LC/Q-TOF systems, Agilent Technologies, Santa Clara, CA), and fluorescence spectroscopy (Quantamaster, Photon Technology International, Inc.). As shown in Fig. SI 1,† we confirmed the presence of two dyes (attributed to 9,10-diphenylanthracene that emits blue light and 2,4-di-*tert*-butylphenyl 1,4,5,8-tetracarboxynaphthalene diamide that emits deep red light).[44] In addition, we confirmed the presence of at least 5 additional compounds, including butyl benzoate, butyl citrate, tributyl acetylcitrate, tri-*n*-butyl aconitate and bis[3,4,6-trichloro-2-(pentyloxycarbonyl)phenyl] oxalate. It is also important to mention that, unlike the response obtained with luminol/H_2O_2 (ref. 38) or $Ru(bpy)_3^{2+}$/tripropylamine[45] that can be rapidly turned on and off, the co-reactants and catalysts contained in the glow sticks can be selected to provide a much longer luminescence.[42,43]

Paper-based devices

Devices were designed using CorelDraw X6 (Corel Corp., Ottawa, Canada) and then cut using a CO_2 laser engraver (Mini 24, 30 W, Epilog Laser Systems, Golden, CO, USA).[46] The μPADs used were fabricated by using Whatman 3MM chromatography paper (VWR International, Radnor, PA, USA). The final design (Fig. 1a) features a circular detection spot (diameter of 4.5 mm, where the ECL reaction took place) and a square sample spot (20.25 mm^2, where the analyte was dispensed). A small channel, width of 1.5 mm and length of 4 mm, was used to connect these two spots while preventing the solutions in each spot from mixing.

Electrode fabrication

ITO electrodes (20 Ω Sq^{-1} or 100 Ω Sq^{-1}) were purchased from Nanocs, NY, USA and were used to benchmark our system against a previous report.[38] Carbon paper (Freudenberg H23C6) was purchased from FuelCellsEtc, TX, USA. Pyrolyzed paper electrodes were prepared as previously reported by our group[47] by pyrolyzing chromatography paper using a Lindberg Blue M tubular furnace (Thermo Scientific; Dubuque, IA) under a controlled atmosphere. Carbon paint electrodes (CPE) were prepared by dispensing 2 mL of carbon paint (E3178, Ercon Inc.; Wareham, MA) on top of a regular microscopy glass slide (25 × 76 mm) and letting it dry overnight in a convection oven at 40 °C.[48] The selected dimensions allowed placing multiple devices in parallel for multiplex sensing. Resistivity measurements of these electrodes were performed using a Keithley 2636A

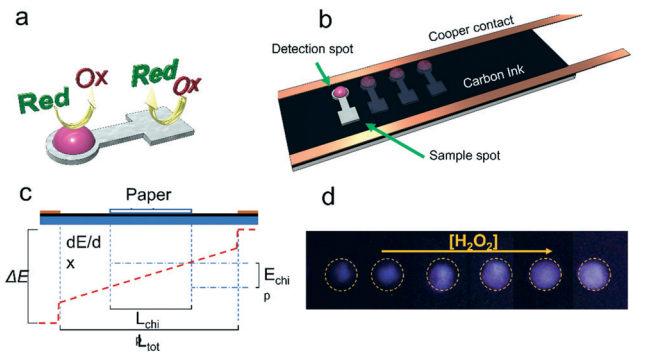

Fig. 1 Schematic representation of the sensor including the principles of SEES. a) Scheme of the paper device indicating the reactions occurring in each spot, b) general overview of the SEES-ECL proposed method, c) diagram showing electrical potential along the electrode, d) real captures of the ECL response using the smartphone. Conditions: 25 V, sample volume: 2.5 μL, [H_2O_2] 0.05–150 mM.

SourceMeter coupled to a Jandel cylindrical four-point probe (Leighton Buzzard, England).

In all cases, a 3 mm conductive copper tape (Sparkfun Electronics, Niwot, CO, USA) was placed along both long edges of the electrode (Fig. 1b) to ensure a uniform electrical contact between the carbon paint electrode and the power supply. Similar to the situation described by Du *et al.*[21] and as shown in Fig. 1c, the potential applied to the contacts (ΔE) induced the circulation of current through the carbon electrode and the development of a uniform electric field across the electrode. When a paper device soaked in electrolyte was placed on the carbon, a small fraction of the current was diverted through the device, driving the electrochemical reactions at the two ends of the paper device.

Image capture

In all cases, the ECL intensity was calculated from images obtained with a Motorola G plus (48 megapixels built-in camera) smartphone and the phone's native application in manual mode. While similar approaches have been previously described,[49,50] images related to this application were obtained setting the white balance to fluorescent mode, the capture time to 8 s and the ISO value to 3200 (maximum sensitivity). The capture was started 15 s after the power supply was turned on and another capture (in normal mode, flash on) at the end of the experiment to image the paper device and identify the region of interest. Representative images of the luminescence obtained are shown in Fig. 1d.

To limit the effect of stray light, an *ad-hoc* box was built using black plexiglass. The box also enabled fixing the position of the smartphone with respect to the single electrode. The parts for the box were cut using a CO_2 laser engraver following guidelines from a previous report.[51] As shown in Fig. SI 2,† the box allowed placing the camera 85 mm away from the surface of the device, which was determined as the minimum distance required to focus on the surface of the electrode. The box was mounted on a plexiglass base that fixed the position of the microscope slide with respect to the cell phone's camera. An additional opening was made at the bottom of the box to enable the electrical connection between the electrode and the power supply. Images were processed using ImageJ software (**https://imagej.nih.gov/**). The process started with the identification of the regions of interest (ROI) of every paper chip using the flash-illuminated capture. Once all the regions were placed with the ROI manager function, the picture color channels were split into the corresponding red, green, and blue channels (Fig. SI 3†). Then, a measure of each ROI was done using the RGB measure tool. It is important to mention that although the luminescence emitted by the glow stick looks pink to the naked eye, the camera in the cell phone does not provide the same sensitivity across the spectrum,[52,53] resulting in purple-tinted pictures. The data were then transferred to a spreadsheet and plotted using OriginPro 2016 software (OriginLab Corporation; Northampton, MA). In all figures, the datapoints and error bars represent the average and standard deviation, respectively, of at least 3 independent measurements.

Measurement procedures

In all cases, the selected electrode was first placed on the plexiglass base and then connected to the power supply (30 V DC, 10 Amp, CSI3010SW, Circuit Specialists; Tempe, AZ). Then, the paper devices were placed on the electrode surface in the normal position with respect to the electric contacts of the single electrode. Unless otherwise stated, the circular extreme of the paper chip was oriented towards the anode (positive pole). Then, 6 μL of electrolyte (0.2 M NaOH, 1 M KCl, and 0.2 M Triton-X) were deposited in the middle of the device, allowing the solution to wet the entire device by simple wicking. Then, 1 μL of dye contained in the glow stick was dispensed on the middle of the round spot of the paper device (facing the anode). Because the paper device was pre-wetted with the aqueous electrolyte, the hydrophobic solution containing the dye remained on top of the paper device. Then, 2.5 μL of the selected analyte sample (*i.e.* hydrogen peroxide, edible oil, or glucose) were dispensed on the square spot of the paper device facing the cathode. This sequence minimized the possibility for the sample to mix with the detection reagents. Next, the system was covered with the plexiglass box, the cell phone was placed on top with the camera facing the device, and the application to capture the images was started. Finally, and unless otherwise noted, the power supply was turned on and 15 s later, a photograph was obtained (8 s exposure) to record the ECL response, followed by a final, flash-illuminated image to record the position of the paper device with respect to the field of view. For the experiments targeting the detection of glucose, 1 μL of a solution containing glucose oxidase (1 mg mL^{-1} dissolved in citrate buffer, pH = 6.0) was placed in the middle of the sample reservoir (square spot) and allowed to interact with the cellulose for 10 min at room temperature.[54] After that, the previously-described procedure was applied for the measurements, noting that pre-wetting the sample spot with the buffer containing the enzyme prevented the penetration of the alkaline electrolyte. Validation of the results, corresponding to real samples, was performed by comparison with reference methods (mFOX method[55] for the peroxides in edible oils and a colorimetric method for the quantification of glucose[56]).

3. Results and discussion

ECL detection

To demonstrate the feasibility of our system to perform ECL, the effect of potential applied (on/off) on the ECL intensity was investigated using 2.5 μL of a solution containing 0.15 M H_2O_2 as the sample. The results (Fig. 2) showed that unless the potential was applied to the system, no luminescence was developed. In contrast, when the power was on, a sharp increase in the ECL intensity was observed, reaching a maximum intensity at approximately 20 s. This value remains constant for a few seconds and then begins to gradually

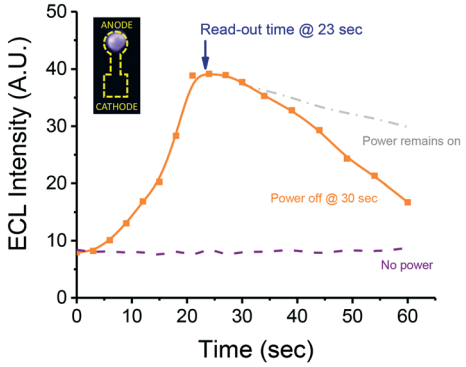

Fig. 2 ECL intensity as a function of time, comparing the response of the device when no power was applied (control), when power was applied for only 30 s, or when power was applied for 60 s. The inset shows a picture showing the position of the detection spot with respect to the paper device. Conditions: E_{tot} = 25 V, sample volume = 2.5 μL, [H_2O_2] = 150 mM, device length = 12 mm.

decrease. It is worth noting that the decrease in ECL (after 25 s) was observed either with or without the power source connected, an issue that was attributed to a combination of dehydration of the device and the consumption of the oxidant. In order to identify the most convenient exposition time that will balance sensitivity towards ECL and analysis time, a series of photographs were collected using the described conditions and after connecting the power supply for 15 s (data not shown). While short exposition times (between 1/30 and 4 s) allowed us to follow the kinetics of the process, they also provided less intensity, limiting the sensitivity of the system. On the other hand, our results showed that longer exposures (*i.e.* between 16 and 32 s), lead to overexposed images that often exceeded the operational time of the paper devices. As a compromise, an exposure of 8 s was selected as optimal and used for all subsequent experiments. These experiments not only allowed for the confirmation of ECL (*vs.* direct reaction with H_2O_2) as the mechanism leading to the emission of light but also selecting 23 s (15 s activation + 8 s capture) as the optimum read-out time.

As a secondary control experiment to confirm that the electro-oxidation of the luminophore was responsible for the emission of light (anodic ECL), two paper chips were placed on the carbon electrode, oriented in opposite directions, with the detection spot facing the anode of the cathode. As shown in Fig. 2 (inset), the luminescence was only observed when the detection spot was oriented towards the anodic region of the chip. These results indicate that, unlike other experiments where both the oxidation of the luminophore and the reduction of the analyte occur in either extreme of the same electrochemical cell,[21,38] the two spots of the paper-based device behave like individual hemi-cells which are electrically connected by the electrolyte soaking the stem. Although only the major components of the dyes in the glow stick were identified, these results demonstrate that the luminophore can be electrochemically oxidized without the need of additional co-reactants.

Electrode selection

As previously noted,[38] the material selected for the fabrication of the electrode has a critical effect on the response because its resistivity defines the electric field gradient between the copper contacts. Therefore, five different electrode materials were considered as candidates for the proposed SEES-ECL system, including two ITO substrates and three carbon-based substrates (*i.e.* carbon paper, carbon ink, and pyrolyzed paper[47]). In order to compare the performance of these electrodes with respect to their properties, the resistivity of the materials was measured and related to the ECL obtained under identical conditions (Fig. 3a). Generally, we observed that the higher the resistivity of the electrode, the higher the resultant signal. While a detailed explanation can be found elsewhere,[38] these results can be explained considering that the electric field gradient generated is distributed between two resistors in parallel, corresponding to the carbon paint electrode or the paper device (soaked with electrolyte). Because both resistors experience the same potential difference, the current circulating through the paper device (which drives the electrochemical reactions) is inversely proportional to the relative resistance of the substrate. Among the substrates evaluated, carbon paper (Freudenberg H23C6, 0.69 ± 0.01 Ω sq^{-1}) and pyrolyzed paper (4.39 ± 0.01 Ω sq^{-1}) featured the highest conductivity, leading not only to Joule heating but also to an ECL response that was barely distinguishable from the blank. While the carbon paper (Freudenberg H23C6) is hydrophobic and performed slightly better, the hydrophilic and porous pyrolyzed paper allowed part of the solution from the paper device to leach into the substrate, contaminating the platform and severely impacting the ECL response. Although ITO 20 (22.12 ± 0.01 Ω sq^{-1}) and ITO 100 (89.8 ± 0.01 Ω sq^{-1}) enabled the electrochemical activation of the paper device, a relatively small signal was observed, an issue that was attributed to a combination of the resistivity and the poor electrocatalytic properties of the ITO.[57] Because it featured the highest resistivity (1573 ± 3 Ω sq^{-1}), the electrode fabricated with carbon paint rendered the highest potential gradient (9.04 V cm^{-1}, Fig. SI 4†) which, in turn, allowed more current to circulate through the paper device and produced the highest ECL signal. This potential is consistent with previous literature reports.[38] Based on these results, carbon paint electrodes were selected as the most appropriate one for this study and were used for the remaining experiments.

The effect of the potential applied to the carbon paint electrode on the ECL response was investigated in order to maximize the signal intensity. Only a marginal change in the ECL intensity was observed over a 0–10 V range (Fig. 3b), suggesting that the potential difference developed at the ends of the paper device was simply not sufficient to drive the electrochemical reaction. Over the 10–25 V range, an exponential increase in the ECL response with respect to the potential applied was observed. Above this voltage, however, a

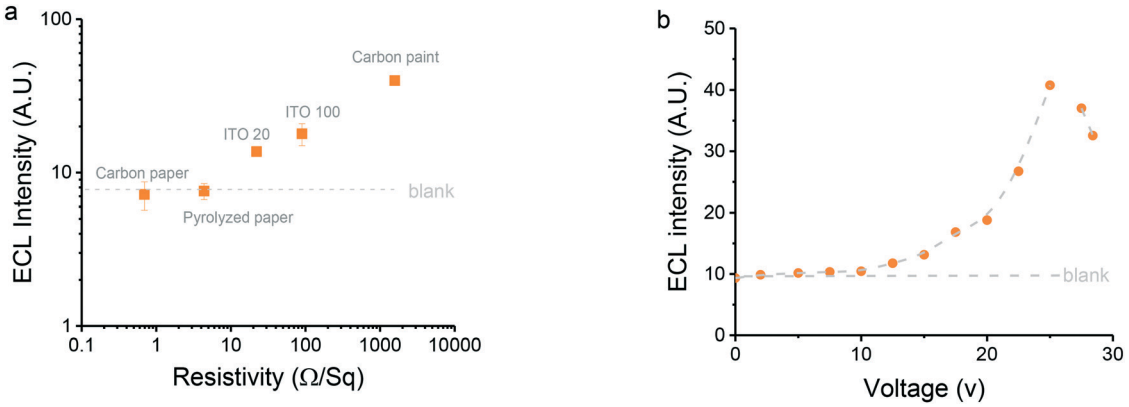

Fig. 3 a: Effect of the material selected for the electrode on the ECL response. Conditions: E_{tot} = 25 V, sample volume = 2.5 μL, [H_2O_2] = 150 mM, read-out time = 23 s, device length = 12 mm. b: Effect of the potential applied to the carbon paint electrode on the ECL response. Conditions: sample volume = 2.5 μL, [H_2O_2] = 150 mM, read-out time = 23 s, device length = 12 mm.

significant drop in the signal intensity was observed, an issue that was attributed to a combination of evaporation of the electrolyte and the fast deterioration of the contacts between the electrode and the paper device. Based on these results, a potential difference of 25 V (9.04 V cm^{-1}, Fig. SI 4†) was selected as the optimal value for the remaining experiments.

Effect of the dimensions of the paper device and sample volume

The paper device was designed to contain the detection system (glow stick dye) and the sample separated by a salt bridge (Fig. 1), used to minimize the chance for direct contact between the solutions by diffusion but allowing the electrical connection between the two spots. Chromatography paper was selected due to its homogeneous color, thickness, and wicking properties,[46] noting that the selection determines the volume of reagents needed and the subsequent electrical and optical response. Thus, considering that the selected electrode produced a potential difference of 9.04 V cm^{-1} (Fig. SI 4†), the effect of the device's length on the ECL response was investigated. A significant increase in the intensity of the ECL response was observed as the length of the device increases from 8 to 12 mm (Fig. 4). These results can be explained considering the electric field of the substrate underneath the device, where the longer the device, the bigger the potential difference. However, a significantly lower ECL response was obtained in paper devices longer than 12 mm, an issue that was attributed to the evaporation of the electrolyte in the device due to Joule heating. It is important to emphasize that paper chips below 8 mm were not included in the figure because these devices were unable to maintain the detection and samples physically separated.

Studies comparing the intensity of ECL as a function of sample volume were also performed. For these experiments, the devices were pre-wetted with the electrolyte, the detection solution was added, and finally increasing volumes of H_2O_2 were dispensed in the sample spot. A proportional increase in the ECL intensity was observed as the sample volume increased, reaching a maximum when 2.5 μL was added (Fig. 4b). Larger samples simply flooded the sensor leading to lower intensity values. In these cases, a clear chemiluminescence emission was observed in the periphery of the paper device, voiding the analysis.

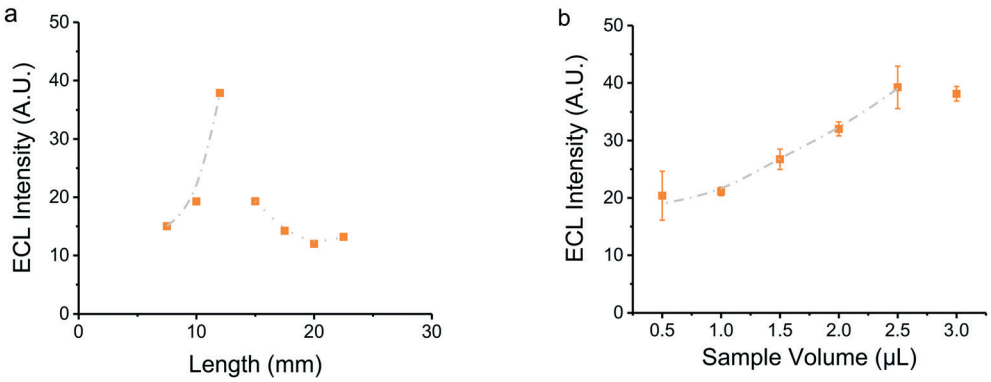

Fig. 4 a: ECL intensity as a function of the length of the paper device. Conditions: carbon paint electrode, E_{tot} = 25 V, sample volume = 2.5 μL, [H_2O_2] = 150 mM, read-out time = 23 s. b: Dependence of the ECL intensity on the volume of the sample added to the sample spot. Conditions: carbon paint electrode, E_{tot} = 25 V, [H_2O_2] = 150 mM, read-out time = 23 s, device length = 12 mm.

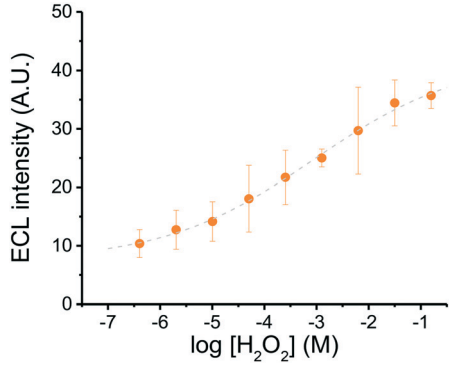

Fig. 5 Calibration curve for hydrogen peroxide as a function of ECL intensity. Conditions: carbon paint electrode, E_{tot} = 25 V, sample volume = 2.5 μL, read-out time = 23 s, device length = 12 mm.

Based on these results, devices with a total length of 12 mm and a sample volume of 2.5 μL were selected as optimal, noting that these values are dependent on the volume of electrolyte (6 μL) used and can be specifically adjusted to fit other applications.

Analytical response

Considering that H_2O_2 is the oxidant contained in most glow sticks, this analyte was initially selected to determine the analytical performance of the system under the previously optimized conditions. Higher concentrations of H_2O_2 led to higher ECL intensities (Fig. 5). From these results, the working range (0.4 μM–150 mM), the limit of detection (LOD, 1.02 μM), and the limit of quantification (LOQ, 3.38 μM) were calculated based on the standard deviation of the background noise.[58] Although these values are comparable with representative examples reported in the literature,[59–63] the proposed approach provides greater versatility and simplicity than traditional systems, including those based on SEES[38,39] and ePADs.[64,65]

In order to use this information to calculate the concentration of unknown samples, the relationship between the ECL response and the $[H_2O_2]$ (in log scale) was also fitted with a sigmoidal function (Boltzmann function, see Fig. 5).

Real sample analysis

To demonstrate its applicability, the proposed methodology was used for two distinct analytical approaches: the direct analysis of peroxides in edible oils and the enzyme-mediated analysis of glucose.

Edible oils contain a mixture of natural saturated and unsaturated fatty acids, triglycerides, phytosterols and phenolic compounds. While the addition of antioxidants can certainly slow the process, exposure of these samples to oxygen and high temperatures leads to the formation of oxidation products such as fatty acid peroxides,[66] altering the quality of these products and potentially affecting the health of consumers. Thus, a number of analytical strategies have been applied to measure the formation of primary/secondary compounds produced or other parameters that can help monitor lipid oxidation.[67–69] In order to facilitate these measurements, the proposed system was applied for determining the peroxides generated in canola oil during mild heating. For these experiments, oil samples (20 mL) were placed in a convection oven (80 °C) and aliquots were taken at different intervals (12 h apart). The peroxide content in the samples was analyzed using the proposed methodology and the ECL responses converted to concentrations using the established calibration curve (Fig. 5). The results showed that longer incubation periods led to higher ECL responses, confirming the formation of the peroxides in the oil samples (see Fig. SI 5†). These findings were validated by analyzing the same samples by the mFOX method.[55] As can be observed in Fig. 6a, a very good agreement between the two methodologies was obtained, highlighting not only the versatility but also the simplicity of the proposed paper-based SEES approach.

To further demonstrate the advantages of the proposed system, an enzyme-mediated analysis was also performed. While it should be noted that the approach is not intended

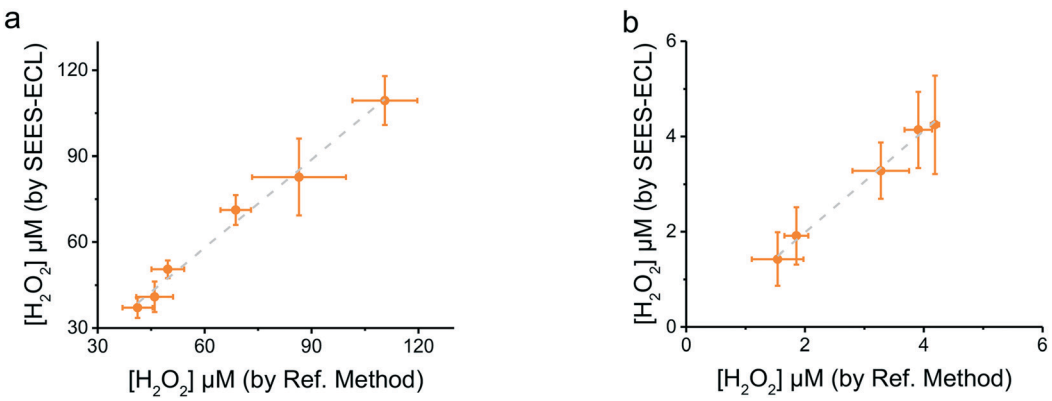

Fig. 6 a: ECL intensity of edible oils after the heating process. Conditions: 2.5 μL sample volume, voltage applied 25 volts, 1.2 mm paper length. b: Determination of glucose in soft drinks (1000× diluted) and fruit juice using the proposed SEES biosensor. Conditions: 2.5 μL sample volume, voltage applied 25 volts, 1.2 mm paper length.

to outperform other biosensing platforms, the glucose/glucose oxidase system was selected as a model. In this case, the only modification performed was the addition of 1 μL of a solution containing glucose oxidase (1 mg mL^{-1} dissolved in citrate buffer, pH = 6.0) to the detection spot. Considering that the oxidation of glucose releases H_2O_2 in stoichiometric amounts, the response after addition of standard solutions of glucose was evaluated against the curve developed with H_2O_2 (Fig. 5). The clear overlap between both curves (Fig. SI 6†) confirmed the utility of the proposed system towards the analysis of H_2O_2 whether initially present in the sample or generated from a reaction. Next, the proposed system was applied to determine glucose in different samples, including three different soft drinks, fresh fruit juice and a sample of dehydrated fruit. In order to obtain solutions containing appropriate concentrations of glucose, these samples were either diluted (×1000 times, for the soft drinks) or vortexed for 10 min in buffer (citrate, pH = 6.0). The results from each of these samples (Fig. SI 7†) were validated using a colorimetric method based on a reaction using glucose oxidase and iodine (reading the absorbance at 353 nm).[56] As can be observed in Fig. 6b, a very good agreement between the two methodologies was also obtained, demonstrating the possibility to extend the applicability of the described approach to bioanalysis.

4. Conclusions

A novel, portable, and inexpensive sensor for multiplex determinations was developed using SEES, ECL, and paper based analytical devices. The detection electrode was fabricated using carbon paint and the dye contained in commercial glow sticks was used as the optical reporter. Besides the electrode material, the system was characterized considering the potential applied, the dimensions of the paper device, and the detection step. Under the optimum experimental conditions, a sigmoidal relationship between the ECL signal (that was recorded using a smartphone) and the concentration of H_2O_2 was obtained. These results allowed the application of the system towards other peroxide-dependent reactions including the oxidation of lipids and the enzymatic transformation of glucose. We believe the proposed system, where one single glow stick can provide enough reagent for more than 100 determinations, could allow the development of numerous additional applications and bridge the gap between recreational chemistry and paper-based analytical electrochemistry.

Conflicts of interest

There are no conflicts to declare.

Acknowledgements

Financial support for this project has been provided by a grant from the Clemson University Animal Co-Products Research & Education Center (ACREC), the Department of Chemistry at Clemson University, and the Universidad Nacional del Sur. E. Vidal and C. E. Domini also thank Consejo Nacional de Investigaciones Científicas y Técnicas (CONICET) for the financial support received.

References

1 A. Yakoh, U. Pimpitak, S. Rengpipat, N. Hirankarn, O. Chailapakul and S. Chaiyo, *Biosens. Bioelectron.*, 2021, **176**, 112912.
2 F. Li, Q. Ye, M. Chen, B. Zhou, J. Zhang, R. Pang, L. Xue, J. Wang, H. Zeng, S. Wu, Y. Zhang, Y. Ding and Q. Wu, *Biosens. Bioelectron.*, 2021, **179**, 113073.
3 M. Elbadawi, J. J. Ong, T. D. Pollard, S. Gaisford and A. W. Basit, *Adv. Funct. Mater.*, 2020, **31**, 2006407.
4 G. Zhao, B. Zhou, X. Wang, J. Shen and B. Zhao, *Food Chem.*, 2021, **354**, 129511.
5 B. Fan, Q. Wang, W. Wu, Q. Zhou, D. Li, Z. Xu, L. Fu, J. Zhu, H. Karimi-Maleh and C. T. Lin, *Biosensors*, 2021, **11**, 155.
6 L. Lu, W. Yuan, Q. Xiong, M. Wang, Y. Liu, M. Cao and X. Xiong, *Anal. Chim. Acta*, 2021, **1141**, 83–90.
7 S. Campuzano, R. Barderas, P. Yáñez-Sedeño and J. M. Pingarrón, *Curr. Opin. Electrochem.*, 2021, **28**, 100703.
8 A. Mobasheri, *Biosensors*, 2020, **11**, 11.
9 I. Grabowska, M. Hepel and K. Kurzatkowska-Adaszynska, *Sensors*, 2021, **22**, 161.
10 J. Xu, Y. Ye, J. Ji, J. Sun and X. Sun, *Crit. Rev. Food Sci. Nutr.*, 2021, 1907736.
11 A. Valverde, J. M. Gordón Pidal, A. Montero-Calle, B. Arévalo, V. Serafín, M. Calero, M. Moreno-Guzmán, M. Á. López, A. Escarpa, P. Yáñez-Sedeño, R. Barderas, S. Campuzano and J. M. Pingarrón, *ChemElectroChem*, 2022, e202200055, DOI: **10.1002/celc.202200055**.
12 R. Vinoth, T. Nakagawa, J. Mathiyarasu and A. M. V. Mohan, *ACS Sens.*, 2021, **6**, 1174–1186.
13 Y. Jiang, Q. Li, Y. Xu, W. Bai, X. Yang, S. Li and Y. Li, *Biosens. Bioelectron.*, 2022, **201**, 113980.
14 Y. Zhao, Y. Xu, L. Shi and Y. Fan, *Anal. Chem.*, 2021, **93**, 11033–11042.
15 S. Wang, L. Zheng, G. Cai, N. Liu, M. Liao, Y. Li, X. Zhang and J. Lin, *Biosens. Bioelectron.*, 2019, **140**, 111333.
16 J. H. Qu, B. Peeters, F. Delport, K. Vanhoorelbeke, J. Lammertyn and D. Spasic, *Biosens. Bioelectron.*, 2021, **192**, 113549.
17 R. Miyan, X. Wang, J. Zhou, Y. Zeng, J. Qu, H. P. Ho, K. Zhou, B. Z. Gao, J. Chen and Y. Shao, *Opt. Express*, 2021, **29**, 31418–31425.
18 T. Ming, Y. Cheng, Y. Xing, J. Luo, G. Mao, J. Liu, S. Sun, F. Kong, H. Jin and X. Cai, *ACS Appl. Mater. Interfaces*, 2021, **13**, 46317–46324.
19 F. Li, L. Guo, Z. Li, J. He and H. Cui, *Anal. Chem.*, 2020, **92**, 6827–6831.
20 S. Emdadi, M. H. Sorouraddin and L. Denanny, *Analyst*, 2021, **146**, 1326–1333.
21 F. Du, Z. Dong, Y. Guan, A. M. Zeid, D. Ma, J. Feng, D. Yang and G. Xu, *Anal. Chem.*, 2022, **94**, 2189–2194.

22 L. Li, Y. Chen and J.-J. Zhu, *Anal. Chem.*, 2017, **89**, 358–371.
23 J. Lu, L. Wang, X. Xu, X. Qin, X. Qiu and Z. Yinggui, *Anal. Methods*, 2019, **11**, 3727–3735.
24 S. A. Kitte, T. Tafese, C. Xu, M. Saqib, H. Li and Y. Jin, *Talanta*, 2021, **221**, 121674.
25 M. M. Richter, *Chem. Rev.*, 2004, **104**, 3003–3036.
26 M. Feng, A. L. Dauphin, L. Bouffier, F. Zhang, Z. Wang and N. Sojic, *Anal. Chem.*, 2021, **93**, 16425–16431.
27 S. Parveen, Y. Chen, Y. Yuan, L. Hu, W. Zhang, M. R. H. S. Gilani, Y. Shi, R. A. Ur and G. Xu, *Sensors and Actuators Reports*, 2021, **3**, 100062.
28 Y. Chen, J. Lin, R. Zhang, S. He, Z. Ding and L. Ding, *Analyst*, 2021, **146**, 5287–5293.
29 C. Aymard, C. Bonaventura, R. Henkens, C. Mousty, L. Hecquet, F. Charmantray, L. J. Blum and B. Doumèche, *ChemElectroChem*, 2017, **4**, 957–966.
30 F. Ben Trad, V. Wieczny, J. Delacotte, M. Morel, M. Guille-Collignon, S. Arbault, F. Lemaître, N. Sojic, E. Labbé and O. Buriez, *Anal. Chem.*, 2022, **94**, 1686–1696.
31 J. Ding, P. Zhou, W. Guo and B. Su, *Front. Chem.*, 2021, **8**, 630246.
32 Y. Luo, F. Lv, M. Wang, L. Lu, Y. Liu and X. Xiong, *Sens. Actuators, B*, 2021, **349**, 130761.
33 X. Ma, W. Gao, F. Du, F. Yuan, J. Yu, Y. Guan, N. Sojic and G. Xu, *Acc. Chem. Res.*, 2021, **54**, 2936–2945.
34 S. Wu, Z. Zhou, L. Xu, B. Su and Q. Fang, *Biosens. Bioelectron.*, 2014, **53**, 148–153.
35 A. Arora, J. C. T. Eijkel, W. E. Morf and A. Manz, *Anal. Chem.*, 2001, **73**, 3282–3288.
36 W. Zhan, J. Alvarez and R. M. Crooks, *J. Am. Chem. Soc.*, 2002, **124**, 13265–13270.
37 K.-F. Chow, F. Mavré and R. M. Crooks, *J. Am. Chem. Soc.*, 2008, **130**, 7544–7545.
38 W. Gao, K. Muzyka, X. Ma, B. Lou and G. Xu, *Chem. Sci.*, 2018, **9**, 3911–3916.
39 X. Ma, L. Qi, W. Gao, F. Yuan, Y. Xia, B. Lou and G. Xu, *Electrochim. Acta*, 2019, **308**, 20–24.
40 M. Bhaiyya, P. K. Pattnaik and S. Goel, *Microfluid. Nanofluid.*, 2021, **25**, 41.
41 M. Okada, I. Nishio, F. Takahashi, H. Tatsumi and J. Jin, *Chem. Lett.*, 2021, **50**, 1659–1661.
42 A. G. Mohan and N. J. Turro, *J. Chem. Educ.*, 1974, **51**, 528.
43 T. S. Kuntzleman, K. Rohrer and E. Schultz, *J. Chem. Educ.*, 2012, **89**, 910–916.
44 The Danish Environmental Protection Agency, 2013, ISBN: 978–87–93026-41-4.
45 K. L. Rahn, T. D. Rhoades and R. K. Anand, *ChemElectroChem*, 2020, **7**, 1172–1181.
46 E. Evans, E. F. M. Gabriel, W. K. T. Coltro and C. D. Garcia, *Analyst*, 2014, **139**, 2127–2132.
47 J. G. Giuliani, T. E. Benavidez, G. M. Duran, E. Vinogradova, A. Rios and C. D. Garcia, *J. Electroanal. Chem.*, 2016, **765**, 8–15.
48 Y. Ding, A. Ayon and C. D. García, *Anal. Chim. Acta*, 2007, **584**, 244–251.
49 J. L. Delaney, C. F. Hogan, J. Tian and W. Shen, *Anal. Chem.*, 2011, **83**, 1300–1306.
50 E. Vidal, A. S. Lorenzetti, C. D. Garcia and C. E. Domini, *Anal. Chim. Acta*, 2021, **1151**, 338249.
51 E. F. M. Gabriel, W. K. T. Coltro and C. D. Garcia, *Electrophoresis*, 2014, **35**, 2325–2332.
52 Y. Ji, Y. Kwak, S. M. Park and Y. L. Kim, *Opt. Express*, 2021, **29**, 11947–11961.
53 S. Tominaga, S. Nishi and R. Ohtera, *Sensors*, 2021, **21**, 4985.
54 L. McCann, T. E. Benavidez, S. Holtsclaw and C. D. Garcia, *Analyst*, 2017, **142**, 3899–3905.
55 S. Dermiş, S. Can and B. Doğru, *Spectrosc. Lett.*, 2012, **45**, 359–363.
56 J. Raba and H. A. Mottola, *Crit. Rev. Anal. Chem.*, 1995, **25**, 1–42.
57 P. Ciocci, J.-F. Lemineur, J.-M. Noël, C. Combellas and F. Kanoufi, *Electrochim. Acta*, 2021, **386**, 138498.
58 M. D. Fernandez-Ramos, L. Cuadros-Rodriguez, E. Arroyo-Guerrero and L. F. Capitan-Vallvey, *Anal. Bioanal. Chem.*, 2011, **401**, 2881–2889.
59 K. Dhara and D. R. Mahapatra, *J. Mater. Sci.*, 2019, **54**, 12319–12357.
60 D.-J. Zheng, Y.-S. Yang and H.-L. Zhu, *TrAC, Trends Anal. Chem.*, 2019, **118**, 625–651.
61 V. Patel, P. Kruse and P. R. Selvaganapathy, *Biosensors*, 2021, **11**, 9.
62 H. Shamkhalichenar and J.-W. Choi, *J. Electrochem. Soc.*, 2020, **167**, 037531.
63 M. Eguílaz, P. R. Dalmasso, M. D. Rubianes, F. Gutierrez, M. C. Rodríguez, P. A. Gallay, M. E. J. López Mujica, M. L. Ramírez, C. S. Tettamanti, A. E. Montemerlo, G. A. Rivas and Curr Opin, *Electrochemistry*, 2019, **14**, 157–165.
64 F. J. V. Gomez, P. A. Reed, D. Gonzalez Casamachin, J. Rivera de la Rosa, G. Chumanov, M. F. Silva and C. D. Garcia, *Anal. Methods*, 2018, **10**, 4020–4027.
65 E. Noviana, C. P. McCord, K. M. Clark, I. Jang and C. S. Henry, *Lab Chip*, 2020, **20**, 9–34.
66 Y. Zhang, M. Wang, X. Zhang, Z. Qu, Y. Gao, Q. Li and X. Yu, *Crit. Rev. Food Sci. Nutr.*, 2021, 2009437.
67 J. Velasco, A. Morales-Barroso, M. V. Ruiz-Méndez and G. Márquez-Ruiz, *J. Chromatogr. A*, 2018, **1547**, 62–70.
68 T. Majchrzak, W. Wojnowski, T. Dymerski, J. Gębicki and J. Namieśnik, *Food Chem.*, 2018, **246**, 192–201.
69 N. Zhang, Y. Li, S. Wen, Y. Sun, J. Chen, Y. Gao, A. Sagymbek and X. Yu, *Food Chem.*, 2021, **358**, 129834.